

Molecular gas in H₂O megamaser active galaxies

F. Raluy¹, P. Planesas¹, and L. Colina^{2*}

¹ Observatorio Astronómico Nacional (IGN), Apartado 1143 E-28800, Alcalá de Henares, Madrid, Spain (raluy@oan.es, planesas@oan.es)

² Space Telescope Science Institute, 3700 San Martin Drive, Baltimore, MD 21218, USA (colina@stsci.edu)

Received 22 September 1997 / Accepted 25 March 1998

Abstract. We have searched for molecular gas towards the nucleus of four galaxies known to harbor a water vapor megamaser. CO(1→0) emission of NGC 2639 and NGC 5506 was strong enough to allow us to map their inner regions. Weak emission from Mkn 1210 was detected and Mkn 1 was not detected at all. We report the tentative detection of the CO(2→1) line in NGC 5506. After this work, 12 of the 18 known galaxies harboring a water vapor megamaser have been observed in CO.

The molecular gas content in the inner regions of water megamaser galaxies ranges from 5×10^7 to $6 \times 10^9 M_{\odot}$. The circumnuclear molecular gas surface density also extends over nearly two orders of magnitude. The maser luminosity is correlated neither with the total amount of molecular gas found in the inner few kpc of these galaxies nor with global properties of the molecular gas such as surface density or filling factor; it is also independent of the infrared and optical luminosities. The only significant correlation we have found involves the maser luminosity and the low frequency radio continuum flux density. We conclude that the maser activity is intrinsically related to the energy of the active galactic nucleus whereas the intensity and even the presence of a water megamaser is independent of the molecular gas global properties such as the molecular gas content and surface density in the inner galactic regions.

We have also found a possible anticorrelation between the molecular gas surface density and the rate of the megamaser variations. A higher molecular gas abundance in the inner region could lead to higher maser variability because of larger nuclear flux variations due to the more variable gas infall, and/or because of more frequent interactions of the pumping agent with molecular gas condensations.

Key words: galaxies: ISM – radio lines: galaxies – galaxies: individual: NGC 2639; NGC 5506; Mkn 1; Mkn 1210

1. Introduction

The first water megamaser was discovered towards the nucleus of NGC 4945 (dos Santos & Lepine 1979). Strong emission

at 22 GHz was detected, with a luminosity about 100 times higher than that of W49, the most powerful galactic water maser. Until 1985 four additional water megamasers were discovered, towards the nuclei of the Circinus Galaxy, NGC 1068, NGC 4258 and NGC 3079. During the following decade no more extragalactic water megamasers were found. In 1994 a survey towards active galactic nuclei was carried out by Braatz et al. (1994), leading to the discovery of five new water megamasers, doubling the number known to that date. Recently, Braatz et al. (1996) have reported the discovery of 6 additional water megamasers towards active galactic nuclei. The last ones up to now have been found in NGC 5793 (Hagiwara et al. 1997) and in NGC 3735 (Greenhill et al. 1997b).

Water megamasers, unlike the galactic and normal extragalactic masers, have been detected at the nuclei of distant galaxies. Interferometric observations (Claussen & Lo 1986; Greenhill et al. 1995a; Greenhill et al. 1996) have shown that megamaser emission comes from within a region around the galactic nucleus whose radius is in general smaller than 1 pc. Another important point is that all the galaxies harboring a water megamaser present some level of activity. This fact has led to suppose that the maser emission mechanism is identical to galactic masers. The huge difference in the energy involved is explained in terms of the pumping source: the energy source of the megamasers is the central object of the active nucleus, a much more powerful source than the central star powering the galactic masers.

Braatz et al. (1997) have recently examined the conditions for detectability of water megamasers in terms of a variety of properties of the active galaxies, but not including the molecular gas content. It is known (Heckman et al. 1989) that Seyfert 2 have abnormally large quantities of dust and gas if compared with Seyfert 1 galaxies. On the other hand LINER galaxies are thought to be simply extensions of Seyfert 2 galaxies to lower luminosities, photoionized by a weaker AGN spectrum (Osterbrock et al. 1993). Thus, the fact that no water megamasers have been found in Seyfert 1 nuclei, while all of them are in either Seyfert 2 or LINER galaxies seems to indicate that a high concentration of molecular gas in the inner regions of the galaxies is a key parameter for the megamaser emission to be produced.

To check this hypothesis and to find if the properties of the masers are related to those of the molecular gas, we have carried

Send offprint requests to: F. Raluy, (raluy@oan.es)

* On assignment from the Space Science Department of ESA

Table 1. Adopted parameters for the observed water megamaser galaxies

Parameter	NGC 2639	NGC 5506	Mkn 1	Mkn 1210
α_{2000}^a	8 ^h 43 ^m 38 ^s .0	14 ^h 13 ^m 14 ^s .9	1 ^h 16 ^m 7 ^s .25	8 ^h 4 ^m 6 ^s .0
δ_{2000}^a	50°12'20.3''	−3°12'26.7''	33°5'22.2''	5°6'50.4''
Morphological type ^a	SA(r)a	SA pec sp	S	S
Activity ^a	LINER	Sy 2	Sy 2	Sy 2
Heliocentric velocity (km s ^{−1}) ^a	3236	1816	4824	4043
V _{LSR} (km s ^{−1})	3235	1825	4825	4030
Distance (Mpc) ^b	44	24	64	54
Position angle (deg) ^c	140	91	—	—
Inclination (deg)	58	80	56	3
D ₂₅ (arcmin) ^c	1.8	2.8	0.8	0.8
Linear scale (pc arcsec ^{−1})	209	118	312	260
log L _{IR} (L _⊙) ^b	10.21	10.35	—	10.58
log L _{FIR} (L _⊙) ^b	9.95	9.85	—	9.85

^a Obtained from the NASA Extragalactic Database (NED)

^b See more information in the text (Sect. 2)

^c Obtained from the RC3 catalog (de Vaucouleurs et al. 1991)

out a study of the molecular gas content and its properties in several of the water vapor megamasers for which no previous data existed or were incomplete. The megamasers we observed are four of those discovered by Braatz et al. in 1994: NGC 2639, NGC 5506, Mkn 1 and Mkn 1210. In our analysis we have used the available CO data for other water megamaser galaxies found in the literature (Heckman et al. 1989; Planesas et al. 1989; Sahai et al. 1990; Aalto et al. 1991; Wang et al. 1992 and Young et al. 1995).

2. Observations

Most of the observations were carried out with the IRAM 30 m radiotelescope at Pico Veleta (Spain) in July 1995. The transitions CO(1→0) at 115 GHz and CO(2→1) at 230 GHz were observed simultaneously; the main beam diameters were 23'' and 12'' respectively, the main beam efficiencies, η_b , 0.68 and 0.40, and the forward efficiencies, η_{fss} , 0.92 and 0.86. The tentative CO(1→0) detection of Mkn 1210 obtained in this observing run prompted us to observe it again, observation that was carried out with the same instrument in May 1997, the antenna parameters being the same than in 1995.

A 512-channel filter-bank with a resolution of 1 MHz was used, providing a velocity coverage of 1200 km s^{−1} in the CO(1→0) line and 600 km s^{−1} in the CO(2→1) line, wide enough to contain the whole range of the CO emission. The velocity resolution was 1.3 km s^{−1} at 230 GHz and 2.6 km s^{−1} at 115 GHz. The focus was checked every few hours correcting it when necessary. Pointing was tested every 2 hours, only small errors were found, 2 – 6''. The typical observing time for each individual point was 2 hours.

All observations were made nutating the subreflector at a rate of 1 Hz, to a position 4' in azimuth from the observed point. Thus, we were able to obtain the flat baselines required for the detection of the wide lines expected towards the inner regions of these galaxies. Linear baselines have been subtracted from each spectrum. To obtain the absolute calibration of the temper-

ature scale, spectra towards IRC+10216 and Orion IRC2 at the redshifted frequencies were taken and compared with the IRAM 30 m catalog of calibrated molecular lines (Mauersberger et al. 1989). The temperature scale in figures is the antenna temperature corrected for atmospheric attenuation and rear spillover, T_A^* . The CO luminosities and derived parameters have been converted to the T_R^* temperature to allow compatibility with the data obtained from the literature.

The adopted parameters for the galaxies we observed are shown in Table 1. Distances were determined from V_{LSR} and a Hubble constant of 75 km s^{−1} Mpc^{−1}. Infrared and far-infrared luminosities were computed using the expressions given in Perault (1987). Isotropic maser luminosities are given in Table 2. Due to the strong temporal variability of the emission, they are only valid for the epoch its observation was carried out.

3. Observational results

3.1. CO(1→0) line

The spectra obtained towards the central regions of the three detected galaxies are shown in Fig. 1. No emission was detected towards Mkn 1 down to a rms noise of 10 mK for a resolution of 42 km s^{−1}. The spectra of NGC 2639 and NGC 5506 are both double peaked. In NGC 2639 the centroid of the CO emission is at V_{LSR} = 3258 km s^{−1} rather similar to the LSR velocities derived from optical observations (3163 km s^{−1}) or from the HI 21 cm line observations (3298 km s^{−1}). In NGC 5506 the LSR velocity is 1827 km s^{−1} from optical observations, 1813 km s^{−1} from HI 21 cm line observations whereas the CO(1→0) centroid velocity is about 1880 km s^{−1}. In Mkn 1210 the centroid velocity of the single fitted Gaussian function appears at V_{LSR} ≈ 3995 km s^{−1} in good agreement with values determined from optical observations (3968 km s^{−1}) or from the HI 21 cm line observations (3978 km s^{−1}). The intensity is 20 mK and the rms noise is 4 mK for a resolution of 21 km s^{−1}.

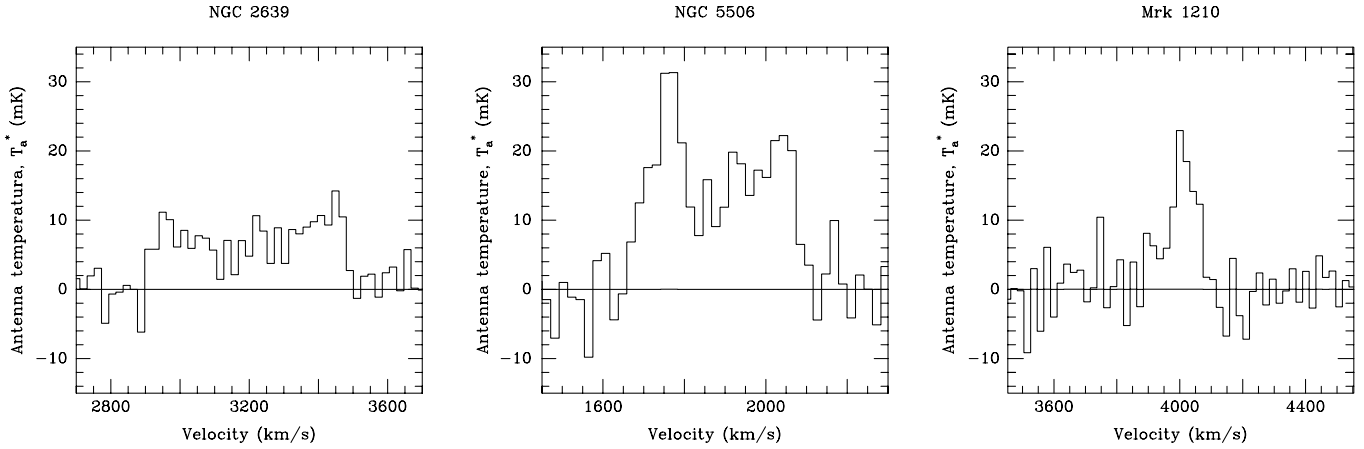


Fig. 1. CO(1→0) emission profiles towards the central region (23'' diameter) of the three detected water megamaser galaxies. Velocity resolution is 21 km s⁻¹. The two NGC objects show double peak spectra, which may indicate the existence of a molecular gas ring surrounding the central AGN at a kpc scale. The spectrum of Mkn 1210 is single-peaked, a possible indication that the expected molecular gas ring is seen face-on. This spectrum was obtained in May 1997

Small maps of NGC 2639 and NGC 5506 were obtained (Fig. 2). The typical rms noise for the thirteen NGC 2639 spectra is between 2 and 7 mK. The mapped region has a diameter of 40'' which corresponds to a size of 8 kpc. The emission is extended in the direction NW–SE, in agreement with the position angle of the galaxy (140°). The distribution of the integrated emission has an elliptical shape with major and minor axis of 30×16'' or 6×3.2 kpc, in agreement with the 58° inclination angle of the galaxy.

For NGC 5506, in addition to the center we observed four positions 20'' away from the nucleus. The rms noise lies between 4 and 6 mK. The observed region is about 60'' in diameter which corresponds to a size of about 7 kpc at the source distance. The emission is more extended towards the E–W direction, in agreement with the position angle of the galaxy (91°).

3.2. CO(2→1) line

Observations of the CO(2→1) line were carried out simultaneously to those of the CO(1→0) line. We obtained a 13-point map of NGC 2639, a 5-point map of NGC 5506 and single central spectra in Mkn 1 and Mkn 1210. The rms noise achieved was 4 mK in the NGC 2639 and Mkn 1210 spectra and 40 mK in that of Mkn 1.

We detected tentatively only the central region of NGC 5506. The rms noise, for a resolution of 21 km s⁻¹, is 8 mK and the line integrated intensity 5.5 K km s⁻¹. The centroid of the CO(2→1) emission is at 1870 km s⁻¹. In Fig. 3 (right panel) the CO(2→1) spectrum produced by adding the five spectra obtained for this galaxy is shown. The CO(2→1)/CO(1→0) line ratio in the inner 20'' region is 0.72, showing that the gas is optically thick in ¹²CO and that the excitation temperature is about 8 K (cf. Braine & Combes, 1992).

3.3. CO luminosities

The CO luminosities in Table 3 have been obtained assuming a Gaussian antenna beam, using the expression: $L_{\text{CO}} = 1.13 d_b^2 I_{\text{CO}}$, where I_{CO} (K(T_R^*) km s⁻¹) is the integrated intensity derived from the CO(1→0) spectra and d_b (pc) is the antenna beam width at the source distance.

The H₂ mass has been derived from the CO luminosity using the standard conversion factor found in galactic giant molecular clouds, $M_{\text{H}_2} = 5.8 L_{\text{CO}}$. High gas temperature and high metallicity could lead to an overestimate while high density and photodissociation of CO could lead to an underestimate of the amount of molecular gas, so, we have used the standard conversion as the most adequate choice.

The molecular gas surface density, Σ_{H_2} has been determined for the region of the galaxy included in the antenna beam, except in the galaxies where this size is larger (see Table 2) than the CO effective diameter ($D_{\text{CO,eff}}$, defined as the diameter that contains the 70 % of the total CO emission). In the last case we used the CO effective diameter to calculate the surface density of molecular gas. To determine this size we used the optical diameter D_{25} . From the data of Kenney & Young (1988) where CO effective diameters are given for a set of galaxies, we have found a correlation between $D_{\text{CO,eff}}$ and D_{25} that is roughly independent of the model chosen for the CO emission distribution. The relation is: $D_{\text{CO,eff}} = 0.44 D_{25}$, very similar to that obtained by Young & Scoville (1991).

In Table 2 the parameters related to the molecular gas are shown for the four galaxies we observed as well as for other water megamaser galaxies whose data have been taken from the literature.

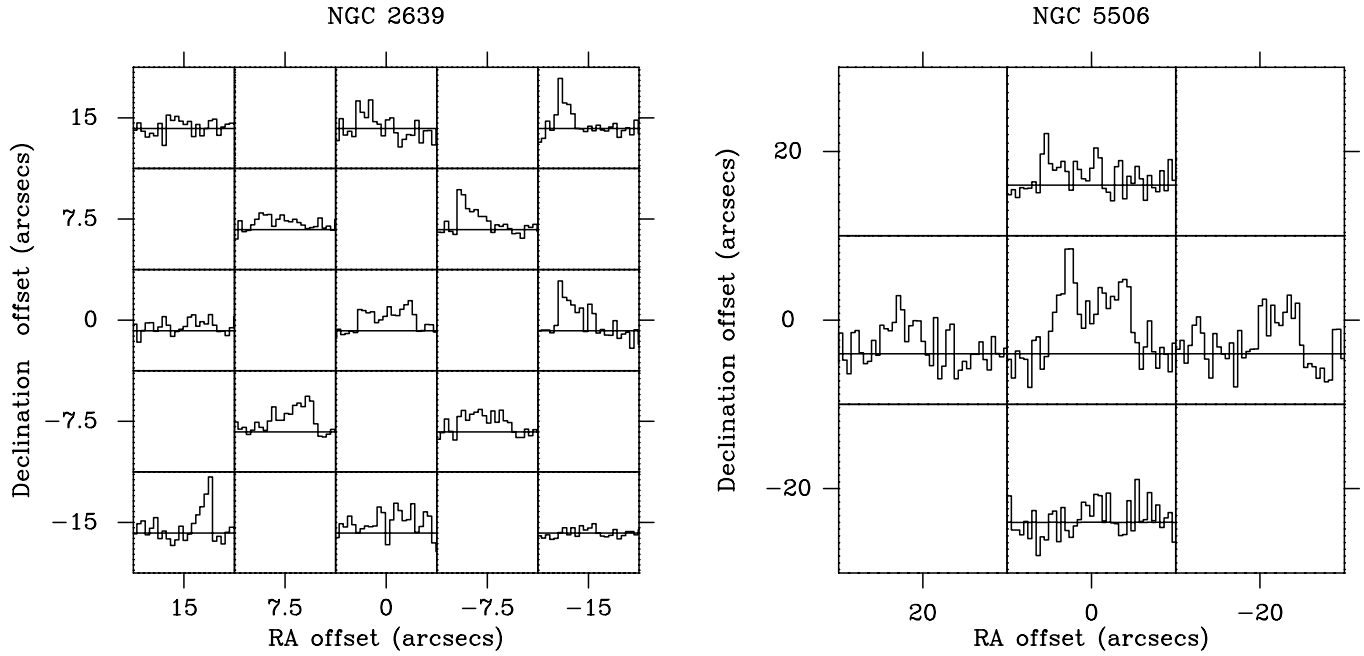


Fig. 2. CO(1→0) maps of the circumnuclear regions of NGC 2639 and NGC 5506. In NGC 2639 the velocity range extends from 2700 to 3700 km s⁻¹ and in NGC 5506 from 1450 to 2300 km s⁻¹. The resolution of the spectra is 21 km s⁻¹ in NGC 5506 and 42 km s⁻¹ in NGC 2639

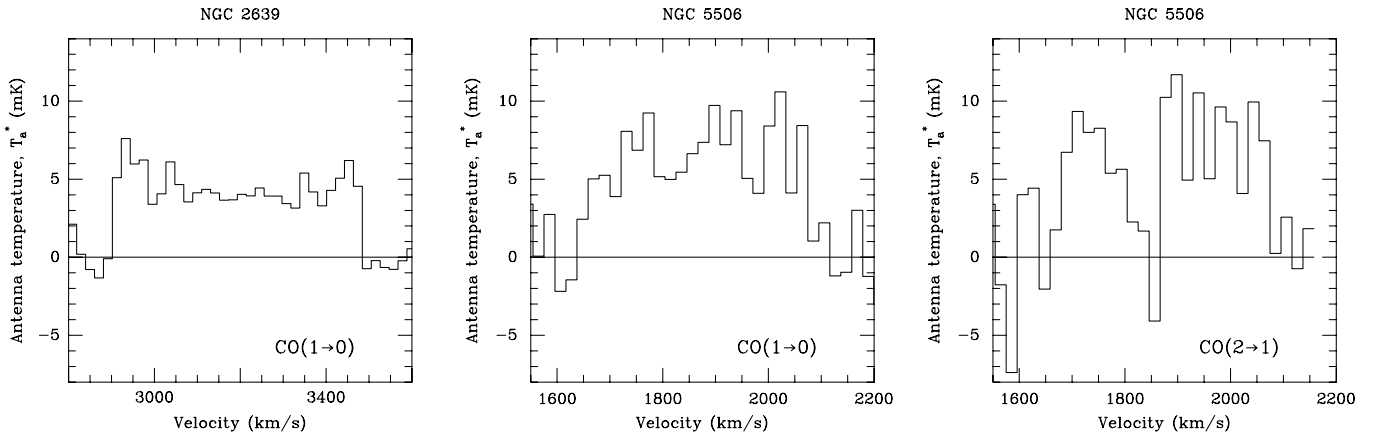


Fig. 3. Left and center panels: CO(1→0) integrated emission of the circumnuclear regions of NGC 2639 and NGC 5506. The spectra have been obtained by adding the individual spectra of all the observed points (5 in the case of NGC 5506 and 13 in NGC 2639). Right panel: CO(2→1) integrated emission of the circumnuclear region of NGC 5506, it has been obtained by adding the spectra of the five observed points. The spectral resolution is 21 km s⁻¹ in all cases. The intensity scale range is also the same, to allow the visual comparison of the intensities. The velocity dispersion in NGC 2639 is very high, the CO(1→0) line has a width of 600 km s⁻¹. In NGC 5506, the emission appears within the same range of velocities (1700–2100 km s⁻¹) for both observed transitions

4. Results

4.1. Mkn 1210

Our data show that Mkn 1210 is a peculiar object among water megamaser galaxies. It has a relatively low surface density of molecular gas, not much higher than that of normal galaxies like the Milky Way or M33. However, its star formation efficiency, estimated from the $L_{\text{IR}}/M_{\text{H}_2}$ ratio, is the highest in our sample. The reason may be that in this kind of objects, a significant fraction (up to 50 %) of the IR luminosity could come from the

active nucleus itself, as is the case for NGC 1068, resulting in an overestimate of the star formation efficiency up to a factor of two.

Nevertheless, there are other indications of a high level of recent star formation activity in this galaxy. The s_{25}/s_{100} ratio (where s_{25} and s_{100} are the IRAS fluxes) has been suggested as the best tracer of the ionizing photon's source (Dultzin-Hacyan et al. 1990). The high measured ratio, $s_{25}/s_{100}=1.59$, in this galaxy would thus indicate a large star formation activity, in spite of the shortage of molecular gas.

Table 2. Molecular gas and maser parameters in the inner region of the water megamaser galaxies

Galaxy	θ_B^a kpc	$D_{CO_{eff}}^b$ kpc	$\log(L_{CO})^c$ K km s ⁻¹ pc ²	$\log(M_{H_2})^d$ M _⊙	L_{IR}/M_{H_2} L _⊙ /M _⊙	$\Sigma_{H_2}^e$ M _⊙ pc ⁻²	I_{max}/I_{min}	Δt years	L_{maser}^f L _⊙
NGC 2639	4.8	10.0	8.1 ¹	8.9	23	21	1.71	1.08	71
NGC 5506	2.7	8.8	7.8 ¹	8.6	56	12	5.43	1.0	61
Mkn 1	7.2	6.6	<8.5 ¹	<9.3	—	—	—	—	64
Mkn 1210	5.7	5.6	7.9 ¹	8.7	84	13	5.0	1.5	99
NGC 1068	0.4	13.0	8.5 ²	9.3	75	61	3.	1.25	170
NGC 3079	3.2	14.9	8.8 ³	9.6	8.4	37	7.	1.25	520
NGC 4258	1.4	15.5	7.4 ³	8.1	34	23	9.0	0.5	85
NGC 4945	1.6	19.6	9.1 ⁴	9.8	9.7	270	1.43	12.5	57
Circinus	1.2	5.1	8.2 ⁴	9.0	—	280	3.13	11.7	24
NGC 1386	2.3	4.9	7.2 ⁵	8.0	30	6.0	—	—	120
NGC 5347	8.9	6.7	8.3 ⁶	9.1	6.7	18	1.33	2.25	32
NGC 1052	1.6	7.6	7.0 ⁷	7.7	38	16	1.75	0.76	140

^a Linear size of the antenna beam at the galaxy distance

^b Effective CO diameter, defined as the diameter that contains 70% of the CO emission (see more details in Sect. 3.3)

^c CO luminosity in the central region of diameter θ_b . Obtained from the CO(1→0) line. Reference numbers correspond to: (1) This paper; (2) Planesas et al. 1989; (3) Young et al. 1995; (4) Aalto et al. 1991; (5) Sahai et al. 1990; (6) Heckman et al. 1989; (7) Wang et al. 1992

^d Obtained using the standard conversion factor found in galactic GMCs, $M_{H_2} = 5.8 L_{CO}$

^e Surface density of molecular gas. It has been obtained for a region whose diameter is the smallest value between θ_b , and $D_{CO_{eff}}$ (see details in Sect. 3.3)

^f Isotropic maser luminosities, taken from Braatz et al. (1996)

4.2. Molecular gas properties and megamaser variability

One of the most interesting properties of water megamasers is their variability. The observations carried out up to now have shown that the megamaser features vary in strength as well as in velocity (e. g. Claussen & Lo, 1986; Greenhill et al. 1995b; Baan & Haschick 1996; Braatz et al. 1996; Hagiwara et al. 1997). These intensity variations can reach a factor of ten. The time scale of the variations range between some weeks and a few years, though Greenhill et al. (1997a) have recently found intensity variations in the Circinus galaxy on a time scale of a few minutes.

We have tried to determine whether long-term time variations could be related somehow to the abundance of molecular gas. The standard AGN model assumes that Seyfert 2 galaxies have a parsec-scale thick torus of gas and dust that blocks the direct view of the nucleus (Antonucci & Miller 1985). In addition to that, a large amount of dense molecular gas has been found in the inner regions of these galaxies (cf. Planesas et al. 1997).

The distribution of this gas could be relevant to the diverse phenomena produced by the interaction of the radiation or matter ejected from the nuclear source. The megamaser phenomenon could arise in the external layers of the nuclear torus, its long-term variability linked to the inhomogeneities of the gas distribution in the external layers of the torus, but could also be affected by other structures that are known to exist in the inner galaxy. In fact, a study of the circumnuclear structure of the galaxy NGC 3079 (Baan & Irwin 1995) showed that there are several structures of molecular gas at different radii from the nucleus.

On the one hand the observed megamaser variations could be related to the intrinsic nuclear variations. Intrinsic variations

at different time scales in radio-continuum flux density have been found in one Seyfert 2 galaxy (NGC 1275, Nesterov et al 1995): slow variations have typical time scales of 20–30 years, faster variations having time scales ranging from some months at millimeter wavelengths to a few years at lower frequencies. All the radio-continuum variations are thought to be produced by changes in the accretion rate of material towards the central black hole. In this case the molecular gas available near the nuclear region (scale of kpc) fuels the accretion disk of the AGN and any variation in the falling rate of gas towards the disk could eventually produce the observed variation in the nuclear radio-continuum emission. The gas present at kpc scales can be transferred to the nuclear region by a kpc-size bar that seems to be very common in spirals (including Seyferts), as shown by NIR observations (Mulchaey et al. 1997). Hence, the presence of molecular gas at a scale of hundreds of parsecs from the nucleus could be significant in the generation of the observed variability of the radio-continuum and therefore of the maser intensity.

Another contribution to the observed megamaser variability could arise from the small structure in the parsec-sized torus or in Giant Molecular Clouds (GMCs) located not far from the nuclear source. In particular, when one of such clouds crosses our line of sight towards the central maser emitting region it could act as an extra amplifier of the emission. The maser variability might be due in part to the inhomogeneity of the molecular clouds, those regions with higher density would produce an increment in the observed maser intensity. Taking a maximum size of 800 AU (Falgarone et al. 1992) for the gas accumulations inside a cloud, and assuming a rotation curve similar to that of NGC 891 (e.g. García-Burillo et al. 1992), the time scale expected for variability produced in this way would be less than

a few tens of years, compatible with the long period variability observed in megamasers. Accepting this reasoning, the 3 year average time-scale of the variability found in water megamasers (cf. Table 2) would be produced by structures ten times smaller.

It could be expected that in both cases, a high abundance of molecular gas in the inner region could lead to a higher variability of the maser, via variable infall rate to the nucleus or via the interaction of the pumping source with inhomogeneous ambient clouds. One of our results agrees with this hypothesis: we have found an anticorrelation (Fig. 4, center panel) between Σ_{H_2} in the central region of water megamaser galaxies and the rate of the relative variations of the megamaser intensity: $(I_{\text{max}}/I_{\text{min}})/\Delta t$, where I_{max} (I_{min}) is the maximum (minimum) peak flux density observed in the megamaser at 22 GHz and Δt is the time elapsed between them. The main objection that can be raised to this tentative result is the low spatial resolution of our determination of Σ_{H_2} , as our measurements include a more extended region than the expected one relevant for the variability of the nuclear source.

4.3. Molecular gas properties and megamaser intensity

From our estimates of Σ_{H_2} we have calculated the number of clouds present in the region we observed, using as the typical GMC parameters a diameter of 40 pc and a mass of $3 \times 10^5 M_{\odot}$ (cf. Wilson et al. 1990). The total volume of the clouds gives us the filling factor in the observed region. Our results show that there is no correlation between the isotropic L_{maser} and the filling factor, see Fig. 4 (left panel). This implies that the total luminosity of the megamaser is not affected by the abundance of molecular clouds in the inner kpc, what is reasonable taking into account that the typical filling factor is ~ 0.01 .

Another naively expected correlation that is not found from our data is that of $\log(L_{\text{maser}})$ vs. Σ_{H_2} . If we suppose that the optical depth of a molecular region is proportional to Σ_{H_2} and that the amplification is exponential: $I = I_0 \exp \tau$ (Baan & Haschick 1996), a dependence between Σ_{H_2} and $\log(L_{\text{maser}})$ is expected. However, as can be seen in the Fig. 4 (right panel) there is no correlation. Due to the complex medium the radiation has to go through it would not be strange that global amplification is far from exponential. Moreover, most of the amplification is likely to take place in a much smaller scale than the one considered when estimating Σ_{H_2} .

4.4. Energy of the central source and maser luminosity

We have not found any correlation (see Fig. 5) between L_{maser} and any other relevant luminosity (i.e., L_{FIR} , L_{IR} , L_{B} , L_{X}). This is surprising, as a closer relationship between L_{FIR} and L_{X} with L_{maser} could be expected. On the one hand, the FIR radiation is thought to be re-emission by molecular and dust clouds of the high energy radiation coming from the central source. On the other hand, the adequate pumping conditions are thought to be produced by the heating of the clouds by X-ray shocks. Therefore, although one would expect the maser luminosity to

be related to the energy release by the central source, this is not the case.

A better measure of the intensity of the central source could be the radio continuum emission. We searched for a correlation between the maser luminosity and the absolute low frequency radio continuum flux density of the galaxies. The radio continuum emission is the sum of nuclear source emission plus the extended emission associated with star formation; however, most of the radio continuum emission in active galaxies comes from the nucleus. Braatz et al. (1997) have found a dependence of the detectability of water megamasers on intrinsic nuclear radio intensity at cm wavelengths. In the lower panels of Fig. 5 L_{maser} is plotted vs. the radio continuum flux data available for the known water megamaser galaxies. Weak correlations are found between L_{maser} and the flux density at 1.4 and 8.4 GHz, although the number of data points at 8.4 GHz is quite small.

From the correlations between L_{maser} and the radio continuum emission at 1.4 and 8.4 GHz may be inferred that the maser luminosity is an intrinsic, energy-related property of the galactic nucleus (which could be characterized by the radio luminosity) rather than by the inner galactic regions (probably best characterized, e.g., by the infrared luminosities and molecular gas abundances).

5. Discussion

We have found no correlation between the maser luminosity and other luminosities, from far-infrared to X-ray luminosity, for a sample of a dozen galaxies, in spite of the presumption that those luminosities could be related in one way or another to the generation or pumping of the maser (cf. Sect. 4.4 and Fig. 5). This result suggests that the maser phenomenon is very localized and is not related to global properties (mass or luminosity) of the galaxies. This is further supported by the correlation found between the low frequency radio continuum and the maser luminosity, both arising mostly very close to the galactic nucleus.

The accumulation of clouds of dense molecular gas around the nucleus of these galaxies seems necessary for the water megamaser to be produced. However, we have found no apparent relation between the maser luminosity and the surface density or the total content of molecular gas in the inner galactic regions (say, the innermost kpc). In spite of that, molecular gas is known to strongly shape the appearance of the central regions of galaxies at different wavelengths. High angular resolution (Martin et al. 1989) and high sensitivity CO maps (Krause et al. 1990) of the water megamaser galaxy NGC 4258 have shown the importance of the molecular gas distribution in confining the radio jets arising from the nucleus. Cecil et al. (1995) have shown the coincidence of the radio jets and soft X-ray jets in this galaxy; the hot gas producing the thermal X-ray jets was interpreted by these authors as shocked gas pulled away from the ambient molecular clouds.

The only possible correlation we have found (Fig. 4, center panel) involves the molecular gas surface density in the inner regions of the galaxies, in the sense that it is anticorrelated with the variation rate of the maser intensity. This result can be inter-

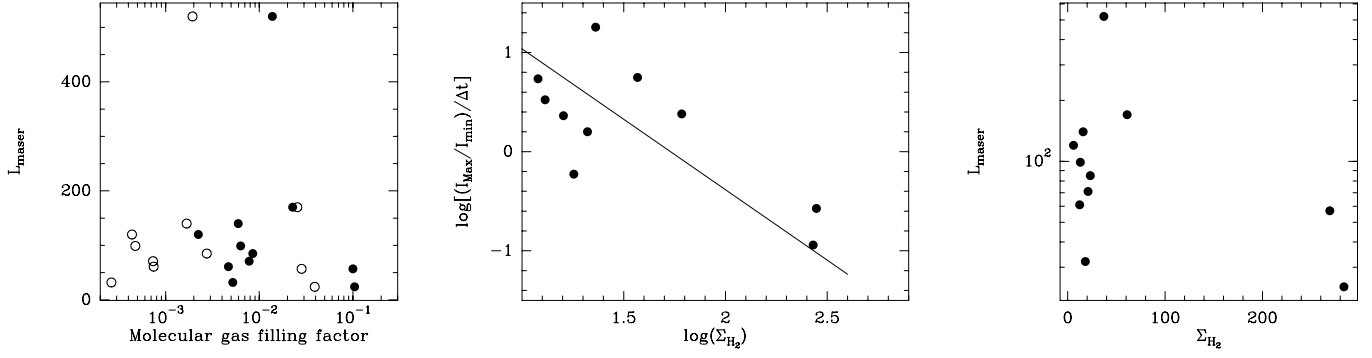


Fig. 4. Maser characteristics vs. molecular gas properties. Left panel: L_{maser} vs. molecular gas filling factor of GMCs (see Sect. 4.3). To estimate the volume filling factor we have considered two cases: (i) a cylindrical geometry (represented in the figure by the black circles) with a diameter the size of the antenna beam at the source distance and a thickness of 300 pc (cf. García-Burillo et al. 1992) and (ii) a spherical geometry (represented by the empty circles) with the diameter of the antenna beam at the source distance. The filling factor is a measure of the probability that a molecular cloud is in the line of sight of the maser. No correlation is found, therefore the isotropic luminosity of the megamaser seems to be independent of the amount of molecular gas present in the central region of the galaxy. L_{maser} is given in L_{\odot} . Center panel: $(I_{\text{max}}/I_{\text{min}})/\Delta t$ vs. Σ_{H_2} ; the first parameter is a measure of the variation rate of the megamaser intensity. There is a possible correlation between the two magnitudes (correlation coefficient of -0.71). Time is given in months and Σ_{H_2} in $M_{\odot}\text{pc}^{-2}$. This result may be affected by the fact that the monitoring of the last discovered megamasers is still incomplete. Right panel: $\log(L_{\text{maser}})$ (in L_{\odot}) vs. Σ_{H_2} (in $M_{\odot}\text{pc}^{-2}$). No correlation is found, see Sect. 4.3

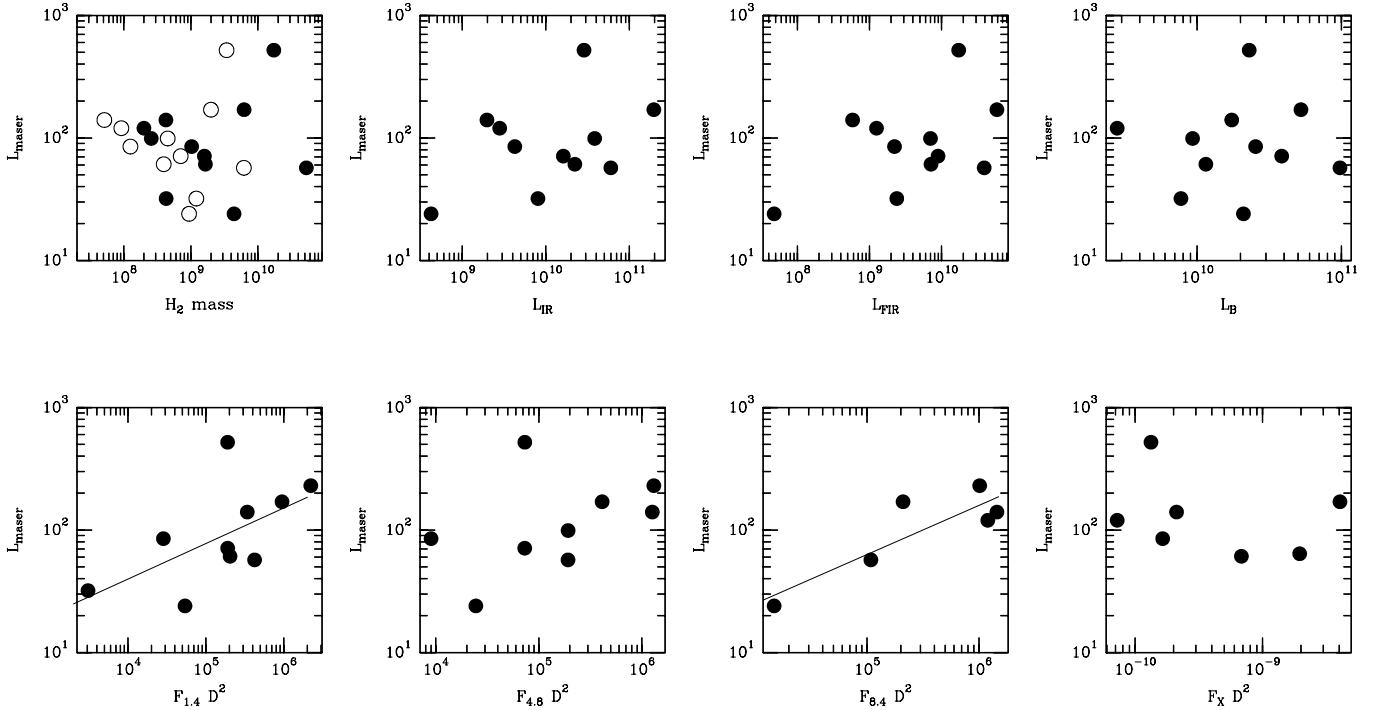


Fig. 5. Plot of L_{maser} vs. several relevant parameters for the water megamaser galaxies. The units of L_{IR} , L_{FIR} and L_{maser} are L_{\odot} , H_2 mass is in M_{\odot} . Radio fluxes are given in mJy, X-ray fluxes in $\text{erg cm}^{-2} \text{s}^{-1}$ and distances in Mpc. There is a certain correlation between the isotropic maser luminosity and the radio continuum flux density at 1.4 GHz and 8.4 GHz (correlation coefficients of 0.6 and 0.87 respectively), see Sect. 4.4

preted in terms of the maser emission being produced or further enhanced by the interaction of the nuclear jets with clouds of matter surrounding the active nucleus at different scales. The combined effect of cloud movement, the small scale structure of the clouds and the intrinsic variability of the central source (itself related to the gas infall towards the nucleus) could ac-

count for the observed variability of the megamaser intensity. This scenario is neither meant to explain maser variability at all time scales, nor all the subtleties observed in water maser variability, but to qualitatively show that one aspect of the variability (its rate of amplitude variations) could be somehow related to the abundance of molecular gas around the nucleus.

6. Conclusions

We have searched for molecular gas towards the nucleus of four galaxies known to harbor a water vapor megamaser, and detected the CO(1→0) emission in three of them and the CO(2→1) emission in one. With this work 12 of the 18 known water megamaser galaxies have been observed in CO, and only the most distant of the observed ones, Mkn 1, has not been detected yet.

1. The 12 water megamaser galaxies with molecular gas data available are not an homogeneous set regarding their molecular gas properties. The amount of H₂ in their circumnuclear regions ranges from 5×10^7 to $6 \times 10^9 M_{\odot}$. The extreme values of the H₂ surface density, Σ_{H_2} , for the central kpc are 6 and $280 M_{\odot} \text{pc}^{-2}$. This parameter extends over a range of 2 orders of magnitude, a range similar to that of Seyfert galaxies, starburst galaxies or luminous infrared galaxies. The maser luminosity, L_{maser} , is not correlated to the total molecular gas mass. Therefore it seems that the total amount of molecular gas in the inner few kpc is not a fundamental parameter on which depends the existence and the average intensity of the water megamaser.
2. L_{maser} is not correlated with Σ_{H_2} or to the filling factor of giant molecular clouds. Apparently the maser luminosity does not depend on the content of molecular gas in the inner kpc. However, the accumulation of clouds of dense molecular gas is believed to be necessary for the generation of a water megamaser. Observations with higher angular resolution of the molecular gas in the inner regions would help to solve the issue.
3. The only correlation we have found involving the maser emission and molecular gas parameters is between the rate of relative variation of the maser intensity and Σ_{H_2} . This fact may indicate that a high abundance of molecular gas in the inner regions could lead to higher variability in the maser emission, on the one hand, due to the higher variability of the central pumping source produced by wider variations in the gas infall; on the other hand, due to the more frequent interactions of the pumping agent with molecular gas condensations.
4. L_{maser} is not correlated to any other luminosity (infrared, optical, X-ray, blue). However, we have found some correlation between L_{maser} and the global radio continuum flux density at 1.4 and 8.4 GHz. This fact supports the idea that L_{maser} is a property related to the galactic nucleus (characterized by the radio luminosities) rather than to the inner galactic regions (characterized by the infrared luminosity and the molecular gas content).
5. Mkn 1210 stands as a peculiar object, having the highest star formation efficiency among water megamaser galaxies in spite of its relatively low molecular gas content.

Acknowledgements. We thank the IRAM staff for their help during our observations at Pico Veleta. We thank the referee, Dr. T. Wiklind for his helpful comments that contributed to improve the paper. P.P. acknowledges partial support by the Spanish DGICYT under project PB93-0048, by the DGES project PB96-0104 and by the Collaborative

Visitor Program at the STScI. F.R. is fully supported by the Spanish DGICYT through the pre-doctoral fellowship FP94 18032957, included in the DGICYT project PB93-0048 and in the DGES project PB96-0104. This research has made use of the NASA/IPAC extragalactic database (NED) which is operated by the Jet Propulsion Laboratory, Caltech, under contract with the National Aeronautics and Space Administration.

References

- Aalto, S., Black, J.H., Johanson, L.E.B., Booth, R.S. 1991, A&A 249, 323
- Antonucci, R.J., Miller, J.S. 1985, ApJ 297, 621
- Baan, W.A., Haschick, A. 1996, ApJ 473, 269
- Baan, W.A., Irwin, J.A. 1995, ApJ 446, 602
- Braatz, J.A., Wilson, A.S., Henkel, C. 1994, ApJ 437, L99
- Braatz, J.A., Wilson, A.S., Henkel, C. 1996, ApJS 106, 51
- Braatz, J.A., Wilson, A.S., Henkel, C. 1997, ApJS 110, 321
- Braine, J., Combes, F. 1992, A&A 264, 433
- Cecil, G., Wilson, A.S., de Pree, C. 1995, ApJ 440, 181
- Claussen, M.J., Lo, K.Y. 1986, ApJ 308, 592
- de Vaucouleurs, G., de Vaucouleurs, A., Corwin, H.G. et al. 1991, Third Reference Catalogue of Bright Galaxies (Springer-Verlag: New York)
- dos Santos, P.M., Lepine, J.R. 1979, Nat. 278, 34
- Dultzin-Hacyan, D., Masegosa, J., Moles, M. 1990, A&A 238, 28
- Falgarone E., Puget J.L., Pérault M. 1993, A&A 257, 715
- García-Burillo S. Guelin, M. Cernicharo, J., Dahlem, M. 1992, A&A 266, 21
- Greenhill, L.J., Jiang, D.R., Moran, J.M. et al. 1995a, ApJ 440, 619
- Greenhill, L.J., Henkel, C., Becker, T.L., Wilson, T., Wouterloot, J. G. A., 1995b, A&A 304, 21
- Greenhill, L.J., Gwinn, C.R., Antonucci, R., Barvainis, R. 1996, ApJ 472, L21
- Greenhill, L.J., Ellingsen, S.P., Norris, R.P. et al. 1997a, ApJ 474, L103
- Greenhill, L.J., Herrnstein, J.R., Moran, J.M., Menten, K.M., Velusamy, T. 1997b, ApJ 486, L18
- Hagiwara, Y., Kohno, K., Kawabe, R., Nakai N. 1997, PASJ 49, 171
- Heckman, T.M., Blitz, L., Wilson, S.A. Armus, L., Miley, G. K. 1989, ApJ 342, 735
- Kenney, J., Young, J.S. 1988, ApJS 66, 261
- Krause, M., Cox, P., García-Barreto, J.A., Downes, D. 1990, A&A 233, L1
- Martin, P., Roy, J.R., Noreau, L., Lo, K.Y. 1989, ApJ 345, 707
- Mauersberger, R., Guélin, M., Martín-Pintado, J. et al. 1989, A&AS 79, 217
- Mulchaey, J.S., Regan, M.W., Kundu, A. 1997, ApJS 110, 299
- Nesterov, N.S., Lyuty, V.M., Valtaoja, E. 1995, A&A 296, 628
- Osterbrock, D.E. 1993, ApJ 404, 551
- Péroullet 1987, Thèse d'Etat, Université de Paris 7
- Planesas, P., Gómez-González, J., Martín-Pintado, J., 1989, A&A 216, 1
- Planesas, P., Colina, L., Pérez-Olea, D. 1997, A&A 325, 81
- Sahai, R., Sundin, M., Claussen, M.J., Rickard, L.J. 1990, Nordic-Baltic Astronomy Meeting
- Wang, Z., Kenney, J.D.P., Ishizuki, S. 1992, AJ 104, 2097
- Wilson, C.D., Scoville, D. 1990, ApJ 363, 435
- Young, J.S., Scoville, N.Z. 1991, ARA&A 29, 581
- Young, J.S., Xie, J. Tacconi, L. et al. 1995, ApJS 98, 219